Electronic Supplementary Material

Flexible, ultrathin, and multifunctional polypyrrole/cellulose nanofiber composite films with outstanding photothermal effect, excellent mechanical and electrochemical properties

Ya-Ge Zhang*, Ling-Zhi Huang*, Qi Yuan (✉), Ming-Guo Ma (✉)

Research Center of Biomass Clean Utilization, MOE Engineering Research Center of Forestry Biomass Materials and Bioenergy, Beijing Key Laboratory of Lignocellulosic Chemistry, College of Materials Science and Technology, Beijing Forestry University, Beijing 100083, China.

E-mails: yuanqixiaowo@163.com (Yuan Q), mg_ma@bjfu.edu.cn (Ma M-G)

* These authors contributed equally to this work.

Electrochemical test

The electrochemical performance of as-obtained samples was assessed by cyclic voltammetry (CV), galvanostatic charge-discharge (GCD), and electrochemical impedance spectroscopy (EIS). The electrochemical measurements were carried out using CHI 760E electrochemical workstation (ChenHua, Shanghai) in 1 M NaCl electrolyte. The above electrochemical tests were all performed under a three-electrode system, in which the PPy/CNF composite films, Ag/AgCl electrode and the Pt sheet were used as the working electrode, reference and counter electrodes, respectively, for the measurement.

The areal capacitance (C_A) was calculated according to the following equations:

$$C_A = \frac{It}{SU} \quad (1)$$

where I (A g^{-1}), t (s), S (cm^2), and U (V) was the current density, the discharging time, the superficial area of the different PPy/CNF films, and the voltage difference of the discharge curve, respectively.

The gravimetric capacitance (C_g) was calculated according to the following equations:

$$C_g = \frac{It}{mU} \quad (2)$$

where I (A g^{-1}), t (s), m (g), and U (V) was the current density, the discharging time, the mass loading of PPy, and the voltage difference of the discharge curve, respectively.

The EIS was measured with a potential amplitude of 10 mV in frequency range of 100kHz to 0.01 Hz.

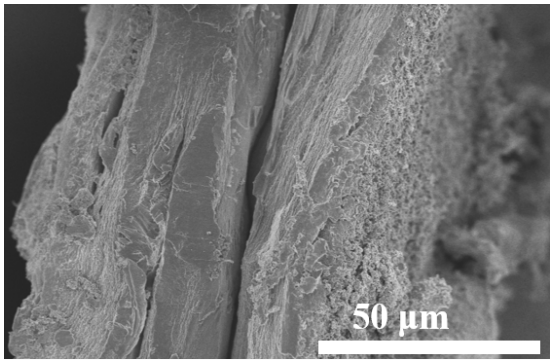

Figure S1. The cross-sectional SEM image of PPy/CNF-3 composite films.

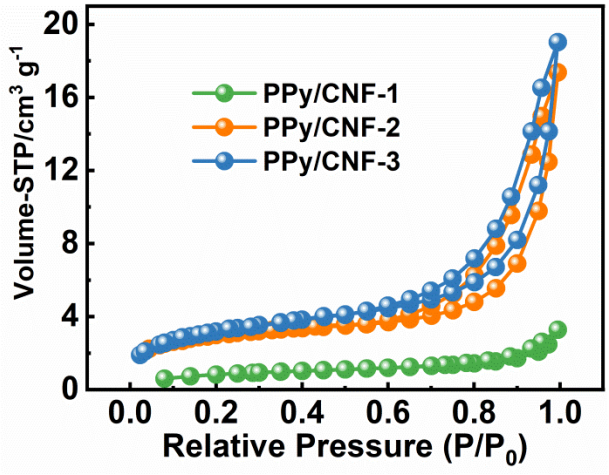

Figure S2. N_2 adsorption/desorption isotherms for the PPy/CNF composite films.

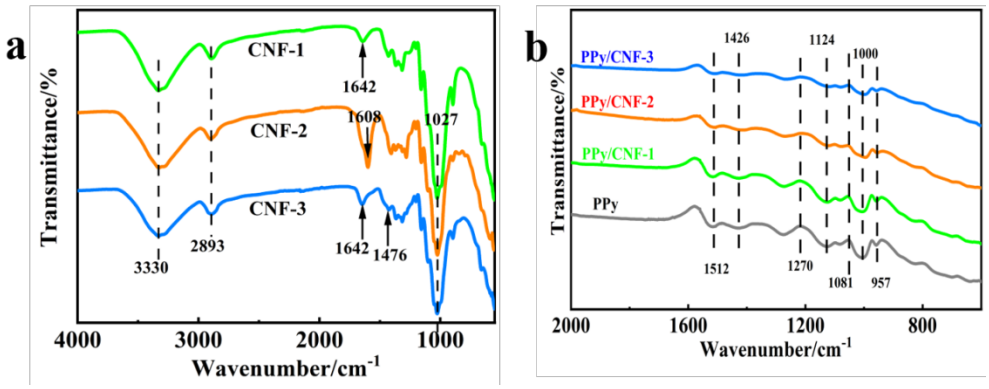

Figure S3. FTIR spectra of the various (a) CNFs and (b) PPy/CNFs.

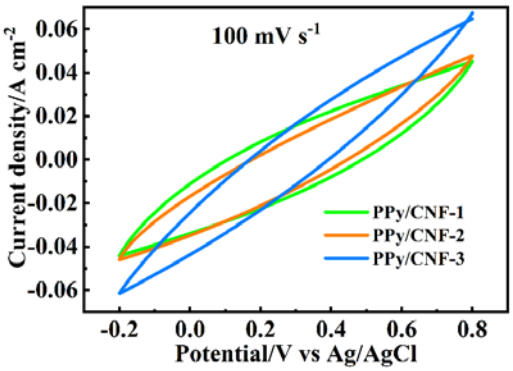

Figure S4. Comparison between cyclic voltammograms (CVs) of PPy/CNF-1, PPy/CNF-2, PPy/CNF-3 composite film electrodes at scan rates of 100 mV s^{-1}.

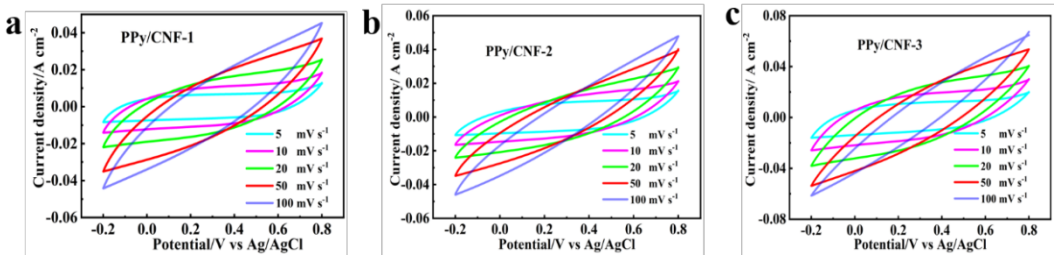

Figure S5. CV curves for the PPy/CNF composite film electrodes at different scan rates of 5, 10, 20, 50, and 100 mV s^{-1}, respectively.

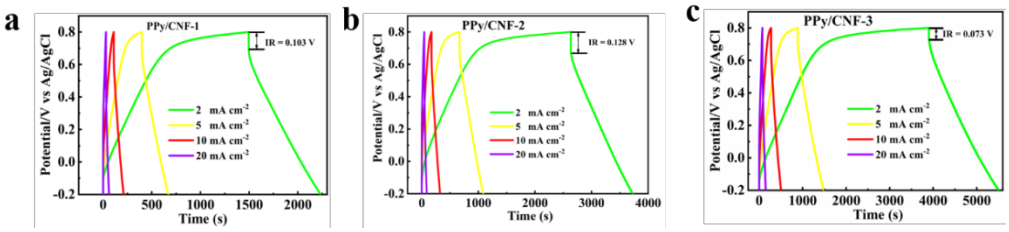

Figure S6. GCD curves recorded at different current densities (2, 5, 10, and 20 mA cm^{-2}) for the PPy/CNF composite film electrodes.

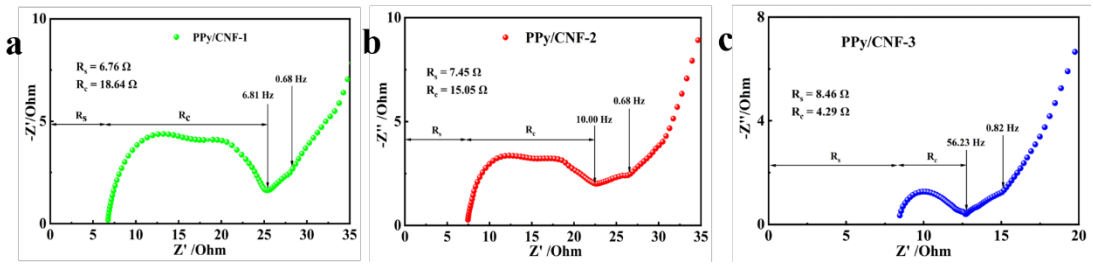

Figure S7. Nyquist plots of the PPy/CNF composite film electrodes.

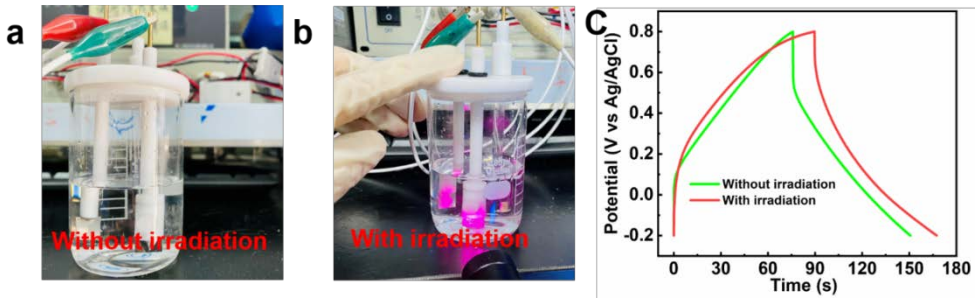

Figure S8. (c) GCD curves recorded at current densities (2 mA cm^{-2}) for the PPy/CNF-3 composite film electrodes under different test conditions with (a) or without (b) near laser irradiation.

Table S1. Compare of specific capacitance and Capacitance retention of PPy/CNF-3 with other recently reported PPy-based SSC.

Electrodes	**Areal capacitance**	**Capacitance retention**	Ref.
PPy@PPNF	156 mF cm^{-2} (1.00 mA cm^{-2})	75% after 5000 cycles	[1]
MXene/BC@PPy hybrid films	200.47 mF cm^{-2} (0.01 mA cm^{-2}))	82.56% after 5000 cycles	[2]
PPy/B-PVA/KCl films	224 mF cm^{-2} (0.8 mA cm^{-2})	—	[3]
PPy@BC/Ti_3C_2Tx composite film	879 mF cm^{-2} (1.00 mA cm^{-2})	83.5% after 10,000 cycles	[4]
TOCN/RGO/PPy film	915 mF cm^{-2} (0.1 mA cm^{-2})	96.6% after 2000 cycles	[5]
Newspaper-based graphite – PPy nano/microcones	1122 mF cm^{-2} (1.00 mA cm^{-2})	87% after 2000 cycles	[6]
PPy/Ag/GO/Cotton fabric	1664.0 mF cm^{-2}(0.5 mA cm^{-2})	—	[7]
PPy/CNF-3	**3.32 F cm^{-2} (1.00mA cm^{-2})**	70% after 5000 cycles	**This work**

References

[1] Lai H R, Bai C R, Wang Y Q, Fan Z Y, Yuan Y, Too H. Highly Crosslinked Conductive Polymer Nanofibrous Films for High-Rate Solid-State Supercapacitors and Electromagnetic Interference Shielding. Advanced Material Interfaces, 2022, 9: 2102115.

[2] Wu Y D, Hu H B, Yuan C Z, Song J, Wu M Z. Electrons/ions dual transport channels design: Concurrently tuning interlayer conductivity and space within re-stacked few-layered MXenes film electrodes for high-areal-capacitance stretchable micro-supercapacitor-arrays. Nano Energy, 2020, 74: 104812.
[3] Sun K J, Feng E K, Zhao G H, Peng H, Wei G G, Lv Y Y, Ma G F. A Single Robust Hydrogel Film Based Integrated Flexible Supercapacitor. ACS Sustainable Chemistry & Engineering. 2019, 7: 165-173.
[4] Song Q C, Zhan Z Y, Chen B X, Zhou Z H, Lu C H. Biotemplate synthesis of polypyrrole@bacterial cellulose/MXene nanocomposites with synergistically enhanced electrochemical performance. Cellulose, 2020, 27: 7475-7488.
[5] Qiang H, He, W, Guo F Y, Cao J Z, Wang R, Guo Z H. Layer-by-Layer Self-Assembled TEMPO-Oxidized Cellulose Nanofiber/Reduced Graphene Oxide/Polypyrrole Films for Self-Supporting Flexible Supercapacitor Electrodes. ACS Applied Nano Materials. 2022, 5: 6305-6315.
[6] Zang L M, Qiao X, Liu Q F, Yang C, Hu L, Yang J, Ma Z H. High-performance solid-state supercapacitors with designable patterns based on used newspaper. Cellulose, 2020, 27: 1033-1042.
[7] Liang C L, Zang L M, Shi F F, Yang C, Qiu J H, Liu Q F, Chen Z M. High-performance cotton fabric-based supercapacitors consisting of polypyrrole/Ag/graphene oxide nanocomposite prepared via UV-induced polymerization. Cellulose 2022, 29: 2525-2537.